Forerunners in bi-gyrotropic materials

Egorov, Igor; Rikte, Sten

1997

CODEN:LUTEDX/(TEAT-7061)/1-28/(1997)
Revision No. 1: April, 1998

Forerunners in bi-gyrotropic materials

Igor Egorov and Sten Rikte

Department of Electroscience
Electromagnetic Theory
Lund Institute of Technology
Sweden

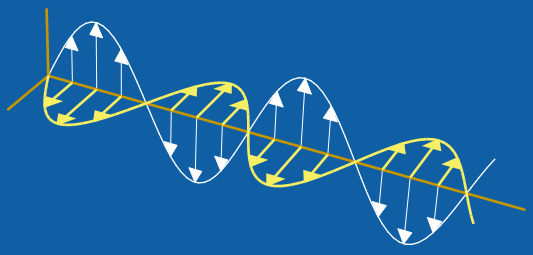

Igor Egorov and Sten Rikte

Department of Electroscience
Electromagnetic Theory
Lund Institute of Technology
P.O. Box 118
SE-221 00 Lund
Sweden

Editor: Gerhard Kristensson

Abstract

Forerunners (precursors) in linear, temporally dispersive, bi-gyrotropic materials are investigated using time-domain techniques. Bi-gyrotropic materials are characterized by twelve constitutive parameters (integral kernels). Specifically, the four susceptibility dyadics are all gyrotropic with a common gyrotropic axis. Pulse propagation along this axis is analyzed using dispersive (noncoupling) wave-splitting and complex time-dependent field vectors. Two numerical examples illustrating the method are presented.

1 Introduction

Material temporal dispersion is an important but, nevertheless, often overlooked phenomenon present at wave propagation in homogeneous dielectrics. Interaction between an electromagnetic pulse and a dispersive medium gives rise to certain characteristic transient fields referred to as forerunners or precursors. Sommerfeld's forerunner (the first precursor) is the leading-edge behavior of the propagating field and is characterized by high frequencies and large amplitudes. Brillouin's forerunner (the second precursor) is due to propagating low-frequency components and arrives later. This precursor is characterized by slow variations and comparatively low amplitudes and contributes significantly to the build-up of the signal. Since all materials are temporally dispersive to some extent, transient phenomena generally cannot be neglected at pulse propagation. The use of ultra-short pulses in applications puts the dispersive response of the medium in focus. This motivates the present study of precursors.

The first descriptions of forerunners were presented by Sommerfeld [28] and Brillouin [3] in the beginning of the 20th century. In these classical works, the saddle-point method was used to analyze the propagation of linearly polarized pulses in single-resonance Lorentz materials. Sommerfeld obtained the first precursor in terms of the Bessel function J_1 with the argument proportional to $\sqrt{zt}$, where z is the propagation distance and t the time measured from the wave front. Brillouin showed that the second precursor can be expressed in terms of the Airy function Ai. Over the years, the theory of precursors has been improved considerably; see, e.g., Oughstun and Sherman [21, 22] and Shen and Oughstun [26]. The traditional way to deal with these problems is the standard Fourier-transform technique: decompose the incident plane pulse into its Fourier components, propagate each such component into the medium, and synthesize the field. The obtained Laplace integral can then be analyzed using asymptotic methods [4, 21].

Attempts have been made to describe transient fields in complex media as well. Zablocky and Engheta [30] studied transverse electric and magnetic pulse propagation in nonabsorbing, isotropic chiral (bi-isotropic) materials. The interest in these materials is due to the new possibilities of design mainly for microwave applications that the additional chirality parameter offers [16]. Knowledge of the performance of transient fields in these materials would be of importance for pulsed radar and ultra-fast laser applications [30]. Zablocky and Engheta decomposed the incident

field in its elementary right-hand circularly polarized (RCP) and left-hand circularly polarized (LCP) components, which, being eigenfields of the chiral medium, can be treated independently, resulting in asymptotic analysis of two Laplace integrals. It was found that a linearly polarized excitation gives rise to precursors, which rotate while propagating through the medium. Moreover, two first and two second forerunners were distinguished in nonabsorbing, single-resonance materials. In the present article, transient fields in lossy isotropic chiral materials are analyzed using time-domain techniques. Pulse propagation in other linear, complex (bi-anisotropic) materials display similar effects, at least when the dynamics of the charges is governed by resonance models. Our ambition is, therefore, to study pulse propagation in general absorbing, complex materials. However, to avoid cumbersome analysis, we restrict ourselves to bi-gyrotropic materials. A linear medium is said to be bi-gyrotropic if all its constitutive dyadics are gyrotropic with a common gyrotropic axis [15]. Bi-gyrotropic materials support transverse electric and magnetic (TEM) waves along the gyrotropic axis. Many interesting materials belong to this group. For instance, isotropic, bi-isotropic, and gyrotropic media are bi-gyrotropic. Optical activity and Faraday effect are two examples of phenomena exhibited by bi-gyrotropic materials.

In recent years, pure time-domain techniques have been used to obtain precursors in stratified complex materials [8, 23]. A time-domain theory of Sommerfeld's forerunner in bi-isotropic media was presented by Rikte [23] and a corresponding theory for anisotropic media was developed by Fridén and Kristensson [8]. The basic idea in these works is that a two-term Maclaurin expansion of the time-dependent susceptibility kernels of the medium would determine the behavior of a propagating pulse shortly after the arrival of the wave front. A time-domain theory of Brillouin's forerunners in dispersive, isotropic dielectrics has been formulated by Karlsson and Rikte [11]. In Ref. 11, the propagating field is expanded in a Taylor series about the observation time. Truncating this series gives successively better approximations to the slowly varying field components in the medium. The present article is aimed to generalize the theory of forerunners presented in Ref. [11] to bi-gyrotropic media.

The outline of the present article is as follows. The problem is formulated in Section 2, where also an account for the variety of bi-gyrotropic materials is given. In Section 3, the basic concepts for discussing the propagation of TEM pulses along the gyrotropic axis of an unbounded bi-gyrotropic medium are introduced. Specifically, a dispersive wave splitting is adopted. Moreover, the fundamental solutions of the first-order, dispersive wave operators associated with the up- and down-going fields are presented. In Section 4, complex, time-varying electromagnetic field vectors appropriate for the problem are introduced. In Section 5, these complex fields are used to obtain the forerunners in the bi-gyrotropic medium. Sommerfeld's forerunner is discussed briefly and Brillouin's forerunner extensively. Two examples illustrating the theory are given in Section 6. Specifically, numerical results for an isotropic chiral medium and for a gyrotropic medium are presented. Numerical techniques are accounted for in Section 7. Conclusions are drawn in Section 8. Finally, in Appendix A, some results for hyper-Airy functions of even orders and complex arguments are given. These functions play a central role in the theory of Brillouin's

forerunner in bi-gyrotropic materials.

2 Problem formulation

In this section, the propagation problem is formulated. Using the dyadic notation in Ref. 15, the constitutive relations of linear, homogeneous, temporally dispersive, bi-anisotropic medium in the absence of an optical response read [10]

$$\begin{cases} c\eta \boldsymbol{D}(\boldsymbol{r},t) = \boldsymbol{E}(\boldsymbol{r},t) + \big(\boldsymbol{\chi}^{ee} * \boldsymbol{E}\big)(\boldsymbol{r},t) + \eta\big(\boldsymbol{\chi}^{em} * \boldsymbol{H}\big)(\boldsymbol{r},t), \\ c\boldsymbol{B}(\boldsymbol{r},t) = \big(\boldsymbol{\chi}^{me} * \boldsymbol{E}\big)(\boldsymbol{r},t) + \eta\boldsymbol{H}(\boldsymbol{r},t) + \eta\big(\boldsymbol{\chi}^{mm} * \boldsymbol{H}\big)(\boldsymbol{r},t), \end{cases} \tag{2.1}$$

where the space- and time-varying electromagnetic field vectors are written as

$$\boldsymbol{F}(\boldsymbol{r},t) = \boldsymbol{u}_x F_x(\boldsymbol{r},t) + \boldsymbol{u}_y F_y(\boldsymbol{r},t) + \boldsymbol{u}_z F_z(\boldsymbol{r},t), \qquad \boldsymbol{F} = \boldsymbol{E}, \boldsymbol{H}, \boldsymbol{D}, \boldsymbol{B}$$

and the time-varying dyadic susceptibility kernels as

$$\boldsymbol{\chi}^{ij}(t) = \sum_{k,l=x,y,z} \boldsymbol{u}_k \boldsymbol{u}_l \chi_{kl}^{ij}(t), \qquad i,j = e,m.$$

Temporal dispersion is modeled by time convolution in the constitutive relations:

$$\big(\boldsymbol{\chi} * \boldsymbol{F}\big)(\boldsymbol{r},t) = \int_{-\infty}^{t} \boldsymbol{\chi}(t-t') \cdot \boldsymbol{F}(\boldsymbol{r},t')\, dt'.$$

(Recall, that the dot product of a dyad $\boldsymbol{ab}$ and a vector $\boldsymbol{c}$ is a vector defined by $\boldsymbol{ab}\cdot\boldsymbol{c} = \boldsymbol{a}(\boldsymbol{b}\cdot\boldsymbol{c})$.) Throughout this article, all dyadics are written in Roman boldface and all vectors in italic boldface. The unit vectors $\boldsymbol{u}_x$, $\boldsymbol{u}_y$, and $\boldsymbol{u}_z$ are the usual Cartesian basis vectors. Standard notation is used for the position vector, $\boldsymbol{r}$, the time, t, the speed of light in vacuum, c, and the intrinsic impedance of vacuum, η. The entries $\chi_{kl}^{ij}(t)$, $i,j = e,m$; $k,l = x,y,z$ of the dyadic susceptibility kernels are zero for $t < 0$ due to causality [10] and assumed to be sufficiently smooth for $t > 0$.

Usually, pulse propagation in dispersive materials and forerunners in particular are discussed for a fixed direction of propagation, $\boldsymbol{u}_z$:

$$\boldsymbol{F}(\boldsymbol{r},t) = \boldsymbol{F}(z,t), \quad \boldsymbol{F} = \boldsymbol{E}, \boldsymbol{H}, \boldsymbol{D}, \boldsymbol{B}. \tag{2.2}$$

This situation arises, for instance, at normal plane-wave incidence on a bi-anisotropic half-space. The analysis of the Maxwell equations at a preferred direction of propagation can be simplified considerably by requiring that all the dyadic susceptibility kernels of the medium commute with the anti-symmetric dyadic

$$\mathbf{J}_T = \boldsymbol{u}_z \times \mathbf{I} = \boldsymbol{u}_z \times \mathbf{I}_T = \boldsymbol{u}_y\boldsymbol{u}_x - \boldsymbol{u}_x\boldsymbol{u}_y,$$

where $\mathbf{I} = \boldsymbol{u}_x\boldsymbol{u}_x + \boldsymbol{u}_y\boldsymbol{u}_y + \boldsymbol{u}_z\boldsymbol{u}_z$ is the identity dyadic and $\mathbf{I}_T = \boldsymbol{u}_x\boldsymbol{u}_x + \boldsymbol{u}_y\boldsymbol{u}_y$. Note that the dyadics $\mathbf{I}_T$ and $\mathbf{J}_T$ are two-dimensional. (Recall that the cross product of a vector $\boldsymbol{a}$ and a dyad $\boldsymbol{bc}$ is a dyad defined by $\boldsymbol{a}\times\boldsymbol{bc} = (\boldsymbol{a}\times\boldsymbol{b})\boldsymbol{c}$.) The intention of

the present discussion can now be formulated precisely: *we wish to establish a time-domain method for propagation of pulses in the preferred direction* $\boldsymbol{u}_z$ *in dispersive bi-anisotropic materials with the commutative property*

$$\boldsymbol{\chi}^{ij}(t) \cdot \mathbf{J}_T = \mathbf{J}_T \cdot \boldsymbol{\chi}^{ij}(t), \qquad i,j = e,m \tag{2.3}$$

in general and forerunners in these materials in particular. (Recall that the dot product of the dyads $\boldsymbol{ab}$ and $\boldsymbol{cd}$ is a dyad defined by $\boldsymbol{ab} \cdot \boldsymbol{cd} = \boldsymbol{a}(\boldsymbol{b} \cdot \boldsymbol{c})\boldsymbol{d}$.) Subjected to the restriction (2.3), the constitutive dyadics can be written as

$$\boldsymbol{\chi}^{ij}(t) = \mathbf{I}_T \chi^{ij}_{\text{co}}(t) + \mathbf{J}_T \chi^{ij}_{\text{cross}}(t) + \boldsymbol{u}_z \boldsymbol{u}_z \chi^{ij}_z(t), \qquad i,j = e,m. \tag{2.4}$$

In other words, these dyadics are all gyrotropic with a common gyrotropic axis, $\boldsymbol{u}_z$, i.e., the medium is bi-gyrotropic [15].

In the actual propagation problem, the four kernels $\chi^{ij}_z(t)$, $i,j = e,m$ do not interfere. The reason for this is that bi-gyrotropic media support the propagation of TEM waves along the gyrotropic axis:

$$\boldsymbol{F}(\boldsymbol{r},t) = \boldsymbol{F}_T(z,t) \equiv \boldsymbol{u}_x F_x(z,t) + \boldsymbol{u}_y F_y(z,t). \tag{2.5}$$

To see this, recall that the Maxwell equations, in response to a current density of the form (2.5) and restricted to solutions of the form (2.2), imply that the longitudinal components of the flux densities are zero; hence,

$$\begin{aligned} 0 = c\eta D_z(z,t) &= E_z(z,t) + \big(\chi^{ee}_z * E_z\big)(z,t) + \eta\big(\chi^{em}_z * H_z\big)(z,t), \\ 0 = cB_z(z,t) &= \big(\chi^{me}_z * E_z\big)(z,t) + \eta H_z(z,t) + \eta\big(\chi^{mm}_z * H_z\big)(z,t). \end{aligned}$$

The longitudinal components of the electric and magnetic fields then satisfy the linear Volterra integral equation of the second kind

$$(\delta + \chi^{ee}_z + \chi^{mm}_z + \chi^{ee}_z * \chi^{mm}_z - \chi^{em}_z * \chi^{me}_z) * F_z = 0, \qquad F_z = E_z, H_z,$$

where $\delta(t)$ is the Dirac delta function. This equation is uniquely solvable in the space of continuous functions in each bounded time interval [13]; consequently, $E_z = 0$ and $H_z = 0$.

Although bi-gyrotropic media only comprises a 12-dimensional subspace of the whole generality of bi-anisotropic materials with 36 degrees of freedom, there are many important classes of materials that belong to this category. These include all isotropic and bi-isotropic materials: dielectric, magnetic, chiral (Pasteur), and nonreciprocal (Tellegen) media [16]. Also uniaxial materials, anisotropic and bi-anisotropic, can be described by the relations (2.1) and (2.4). These include dielectric and magnetic crystals belonging to the tetragonal, hexagonal, and trigonal systems as well as chiral materials with alignment of helices. In addition to these media with symmetric constitutive dyadics, also various nonsymmetric material characterizations are allowed: $\chi^{ee}_{\text{cross}} \neq 0$ for magnetoplasma, $\chi^{mm}_{\text{cross}} \neq 0$ for magnetized ferrite, which are two examples of nonreciprocal bi-gyrotropic materials. A moving medium has the property $\chi^{em}_{\text{cross}} \neq 0$ [27], and an example of a reciprocal material with $\chi^{em}_{\text{cross}} \neq 0$ is the so-called Omega-hat medium, where the magnetoelectric coupling is generated by symmetrically placed Omega-shaped elements [17, 19, 20, 25].

3 Basic equations

In this section, the basic concepts for discussing TEM pulse propagation, (2.5), along the gyrotropic axis, $\boldsymbol{u}_z$, through an unbounded bi-gyrotropic medium are introduced. To simplify the notation, the explicit dependence of the time- and space-coordinates is often suppressed.

3.1 Wave splitting

The Maxwell equations model the dynamics of the electromagnetic fields:

$$\nabla \times \boldsymbol{E} = -\partial_t \boldsymbol{B}, \qquad \nabla \times \boldsymbol{H} = \boldsymbol{J}^e + \partial_t \boldsymbol{D}.$$

In this article, the current density $\boldsymbol{J}^e = \boldsymbol{J}^e_T(z,t)$ is of the form (2.5) and hence gives rise to TEM waves propagating along the gyrotropic axis. Note the difference between the vector $\boldsymbol{J}^e_T$ and the dyadic $\mathbf{J}_T$. Subjected to this excitation, the Maxwell equations reduce to

$$\partial_z \boldsymbol{E}_T = c^{-1}\partial_t \mathbf{J}_T \cdot (c\boldsymbol{B}_T), \quad \partial_z \mathbf{J}_T \cdot (\eta \boldsymbol{H}_T) = c^{-1}\partial_t (c\eta \boldsymbol{D}_T) + \eta \boldsymbol{J}^e_T,$$

where the dyadic identity $\mathbf{J}_T \cdot \mathbf{J}_T = -\mathbf{I}_T$ has been employed. The flux densities, $\boldsymbol{D}_T$ and $\boldsymbol{B}_T$, can be eliminated using the constitutive relations. The remaining dependent vector field variables, the electric field intensity, $\boldsymbol{E}_T$, and the magnetic field intensity, $\boldsymbol{H}_T$, satisfy a system of coupled hyperbolic integro-differential equations:

$$\begin{cases} \partial_z \boldsymbol{E}_T = c^{-1}\partial_t \mathbf{J}_T \cdot (\boldsymbol{\chi}^{me}_T * \boldsymbol{E}_T + \eta \boldsymbol{H}_T + \boldsymbol{\chi}^{mm}_T * \eta \boldsymbol{H}_T), \\ \partial_z \mathbf{J}_T \cdot (\eta \boldsymbol{H}_T) = c^{-1}\partial_t (\boldsymbol{E}_T + \boldsymbol{\chi}^{ee}_T * \boldsymbol{E}_T + \boldsymbol{\chi}^{em}_T * \eta \boldsymbol{H}_T) + \eta \boldsymbol{J}^e_T, \end{cases} \tag{3.1}$$

where $\boldsymbol{\chi}^{ij}_T(t) = \mathbf{I}_T \chi^{ij}_{\mathrm{co}}(t) + \mathbf{J}_T \chi^{ij}_{\mathrm{cross}}(t)$, $i,j = e,m$ are two-dimensional constitutive dyadics.

A generalization of the dispersive wave splitting proposed in Ref. [24] is now adopted. Wave splitting is a change of the dependent vector field variables, such that the new variables, say $\boldsymbol{E}^{\pm} = \boldsymbol{E}^{\pm}(z,t)$, represent the up- and down-going waves in the medium, respectively.

The total electric field is written as the sum of the split vector fields:

$$\boldsymbol{E}_T = \boldsymbol{E}^+ + \boldsymbol{E}^-. \tag{3.2}$$

The total magnetic field is expressed in terms of these fields as

$$\mathbf{J}_T \cdot (\eta \boldsymbol{H}_T) = -\mathbf{Y}^+ * \boldsymbol{E}^+ + \mathbf{Y}^- * \boldsymbol{E}^-, \tag{3.3}$$

where the time-varying dyadics $\mathbf{Y}^{\pm}(t)$ are of the form

$$\mathbf{F}(t) = \mathbf{I}_T \delta(t) + \mathbf{I}_T F_{\mathrm{co}}(t) + \mathbf{J}_T F_{\mathrm{cross}}(t). \tag{3.4}$$

The dyadics $\mathbf{Y}^{\pm}(t)$, which are referred to as *the relative intrinsic admittances of the bi-gyrotropic medium associated with up- and down-going waves along the gyrotropic*

axis, respectively, are specified below. The imposed conditions (3.2)–(3.3) imply that the principal form of the *temporally dispersive wave splitting* is

$$2\boldsymbol{E}^{\pm} = \mathbf{Z} * \mathbf{Y}^{\mp} * \boldsymbol{E}_T \mp \mathbf{Z} * \mathbf{J}_T \cdot (\eta \boldsymbol{H}_T)\,, \tag{3.5}$$

where the time-varying dyadic $\mathbf{Z}(t)$ is of the form (3.4) and satisfies the linear, dyadic Volterra integral equation of the second kind

$$\mathbf{Z} * \left(\mathbf{Y}^{+} + \mathbf{Y}^{-}\right) = 2\delta \mathbf{I}_T.$$

Dyadic Volterra integral equations of the second kind are uniquely solvable in the space of continuous functions in each bounded time interval. Therefore, the dyadic $\mathbf{Z}(t)$, which is referred to as *the relative intrinsic impedance of the bi-gyrotropic medium*, is well-defined.

An appropriate choice of the admittance dyadics $\mathbf{Y}^{\pm}$ reduces the Maxwell equations (3.1) to one first-order integro-differential equation for $\boldsymbol{E}^{+}$ and one for $\boldsymbol{E}^{-}$. To see this, differentiate equation (3.5) with respect to z and substitute (3.1) into the result. Furthermore, let the admittance dyadics $\mathbf{Y}^{\pm}(t)$ be the solutions of the nonlinear, dyadic Volterra integral equations of the second kind

$$(\delta \mathbf{I}_T + \boldsymbol{\chi}_T^{mm}) * \mathbf{Y}^{\pm} * \mathbf{Y}^{\pm} \mp \mathbf{J}_T \cdot (\boldsymbol{\chi}_T^{em} + \boldsymbol{\chi}_T^{me}) * \mathbf{Y}^{\pm} = \delta \mathbf{I}_T + \boldsymbol{\chi}_T^{ee}. \tag{3.6}$$

The dynamical equations for the split vector field variables then become

$$\partial_z \boldsymbol{E}^{\pm} = \mp c^{-1} \partial_t \left(\mathbf{N}^{\pm} * \boldsymbol{E}^{\pm}\right) \mp \left(\mathbf{Z} * \eta \boldsymbol{J}_T^{e}\right)/2, \tag{3.7}$$

where the time-varying dyadics

$$\mathbf{N}^{\pm} = (\delta \mathbf{I}_T + \boldsymbol{\chi}_T^{mm}) * \mathbf{Y}^{\mp} \pm \mathbf{J}_T \cdot \boldsymbol{\chi}_T^{em} \tag{3.8}$$

are of the form (3.4) and are referred to as *the indices of refraction of the bi-gyrotropic medium for up- and down-going waves along the gyrotropic axis*, respectively. Observe that the quantities $\mathbf{N}^{\pm}(t)$, $\mathbf{Y}^{\pm}(t)$, and $\mathbf{Z}(t)$ represent the intrinsic properties of the medium, that is, they are independent of the field vectors and depend on the susceptibility kernels of the medium only. Being solutions of Volterra integral equations of the second kind, these dyadics inherit the properties of the susceptibility kernels; consequently, they are zero for $t < 0$ and smooth for $t > 0$.

The refractive indices can be computed directly from susceptibility data. Combining equations (3.8) and (3.6) yields the nonlinear, dyadic Volterra integral equations of the second kind

$$(\mathbf{N}^{\pm} \mp \mathbf{J}_T \cdot \boldsymbol{\chi}_T^{em}) * (\mathbf{N}^{\pm} \pm \mathbf{J}_T \cdot \boldsymbol{\chi}_T^{me}) = (\delta \mathbf{I}_T + \boldsymbol{\chi}_T^{ee}) * (\delta \mathbf{I}_T + \boldsymbol{\chi}_T^{mm}). \tag{3.9}$$

In particular, for bi-isotropic materials, one obtains

$$\begin{cases} 2N_{\mathrm{co}}^{\pm}(t) + \left(N_{\mathrm{co}}^{\pm} * N_{\mathrm{co}}^{\pm}\right)(t) = \chi^{ee}(t) + \chi^{mm}(t) + \left(\chi^{ee} * \chi^{mm}\right)(t) - (L * L)(t), \\ N_{\mathrm{cross}}^{\pm}(t) = \pm \kappa(t), \end{cases}$$

where $L(t) = (\chi^{em}(t) + \chi^{me}(t))/2$ and $\kappa(t) = (\chi^{em}(t) - \chi^{me}(t))/2$ are the nonreciprocity kernel and the chirality kernel, respectively, which is in concordance with known results [24]. In the achiral case, $N_{\mathrm{cross}}^{\pm}(t) = 0$, cf. Ref. 11.

3.2 Causal fundamental solutions

In this section, the first-order, dispersive vector wave equations (3.7) are studied. Specifically, the retarded fundamental solutions (the causal Green's functions)

$$\mathcal{E}^{\pm}(z;t) = \mathbf{I}_T \mathcal{E}^{\pm}_{\mathrm{co}}(z;t) + \mathbf{J}_T \mathcal{E}^{\pm}_{\mathrm{cross}}(z;t), \tag{3.10}$$

of the dispersive, dyadic wave operators

$$\pm\partial_z \mathbf{I}_T \cdot + c^{-1}\partial_t \mathbf{N}^{\pm} * \tag{3.11}$$

are discussed.

The fundamental solutions satisfy the dispersive dyadic wave equations

$$\begin{aligned}\left(\pm\partial_z + c^{-1}\partial_t\right)\mathcal{E}^{\pm}(z,t) + c^{-1}\left(\mathbf{I}_T N^{\pm}_{\mathrm{co}}(+0) + \mathbf{J}_T N^{\pm}_{\mathrm{cross}}(+0)\right)\cdot\mathcal{E}^{\pm}(z,t)\\ + \left(\mathbf{K}^{\pm}(\cdot) * \mathcal{E}^{\pm}(z,\cdot)\right)(t) = \mathbf{I}_T\delta(z)\delta(t),\end{aligned}$$

where the first term constitutes the free-space contribution, the second term causes attenuation and rotation of the wave front, and the third term reflects material dispersion. The kernels $\mathbf{K}^{\pm}(t)$ are referred to as the *wave-number kernels associated with up- and down-going waves along the gyrotropic axis*, respectively. Explicitly, these kernels are

$$\mathbf{K}^{\pm}(t) = \mathbf{I}_T K^{\pm}_{\mathrm{co}}(t) + \mathbf{J}_T K^{\pm}_{\mathrm{cross}}(t), \tag{3.12}$$

where $K^{\pm}_{\mathrm{co}}(t) = c^{-1}\left\{\partial_t N^{\pm}_{\mathrm{co}}(t)\right\}$ and $K^{\pm}_{\mathrm{cross}}(t) = c^{-1}\left\{\partial_t N^{\pm}_{\mathrm{cross}}(t)\right\}$ are classical time-derivatives.

Under suitable assumptions, Schwartz' kernel theorem [9, pp. 128-129] is applicable, and the solutions of the wave equations (3.7) can be written in the form

$$\boldsymbol{E}^{\pm}(z,t) = -\frac{1}{2}\int\left(\int \mathcal{E}^{\pm}(z-z';t-t')\cdot(\mathbf{Z} * \eta\boldsymbol{J}^{e}_{T})(z',t')\,dt'\right)dz'. \tag{3.13}$$

In the following theorem, the retarded fundamental solutions (3.10) of the dispersive wave operators (3.11) are defined in terms of the wave-number kernels (3.12). The theorem can be proved by straightforward differentiation. The Heaviside step function is denoted by H.

Theorem 3.1. *The distributions,*

$$\mathcal{E}^{\pm}(z;t) = H(\pm z)\mathbf{Q}^{\pm}(\pm z)\cdot\Big(\mathbf{I}_T\delta\left(t\mp z/c\right) + \mathbf{P}^{\pm}(\pm z; t\mp z/c)\Big), \tag{3.14}$$

where the regular wave-front dyadics,

$$\mathbf{Q}^{\pm}(z) = \mathbf{I}_T Q^{\pm}_{\mathrm{co}}(z) + \mathbf{J}_T Q^{\pm}_{\mathrm{cross}}(z),$$

satisfy the ordinary differential equations,

$$c\partial_z\mathbf{Q}^{\pm}(z) = -\left(\mathbf{I}_T N^{\pm}_{\mathrm{co}}(+0) + \mathbf{J}_T N^{\pm}_{\mathrm{cross}}(+0)\right)\cdot\mathbf{Q}^{\pm}(z), \quad \mathbf{Q}^{\pm}(0) = \mathbf{I}_T,$$

and the regular dyadic propagator kernels,

$$\mathbf{P}^{\pm}(z;t) = \mathbf{I}_T P^{\pm}_{\mathrm{co}}(z;t) + \mathbf{J}_T P^{\pm}_{\mathrm{cross}}(z;t),$$

satisfy the integro-differential equations,

$$\partial_z \mathbf{P}^{\pm}(z;t) = -\mathbf{K}^{\pm}(t) - \big(\mathbf{K}^{\pm}(\cdot) * \mathbf{P}^{\pm}(z;\cdot)\big)(t), \quad \mathbf{P}^{\pm}(0;t) = 0, \tag{3.15}$$

are causal or retarded fundamental solutions of the dispersive dyadic wave operators (3.11), respectively. In particular, $\mathbf{P}^{\pm}(z;t) = \mathbf{0}$ *for* $t < 0$.

The dyadics $\mathbf{Q}^{\pm}(z)$ determine the attenuation and rotation of the up- and downgoing wave fronts at the propagation depth z, respectively. Integrating the ODEs for the wave-front dyadics gives

$$\begin{aligned}\mathbf{Q}^{\pm}(z) &= \exp\left(-z\left(\mathbf{I}_T N^{\pm}_{\mathrm{co}}(+0) + \mathbf{J}_T N^{\pm}_{\mathrm{cross}}(+0)\right)/c\right) \\ &= \exp\big(-zN^{\pm}_{\mathrm{co}}(+0)/c\big)\Big(\mathbf{I}_T \cos\big(-zN^{\pm}_{\mathrm{cross}}(+0)/c\big) + \mathbf{J}_T \sin\big(-zN^{\pm}_{\mathrm{cross}}(+0)/c\big)\Big).\end{aligned}$$

Similarly, the integro-differential equations (3.15) for the dyadic propagator kernels, $\mathbf{P}^{\pm}(z;t)$, can be integrated. In operator sense,

$$\mathbf{I}_T + \mathbf{P}^{\pm}(z,\cdot)* = \exp\big(-z\mathbf{K}^{\pm}(\cdot)*\big),$$

where the star denotes dyadic temporal convolution and the exponentials are interpreted in terms of their Maclaurin series, i.e.,

$$\mathbf{P}^{\pm}(z;t) = \sum_{n=1}^{\infty} \frac{(-z)^n}{n!} \left(\left(\mathbf{K}^{\pm}*\right)^{n-1} \mathbf{K}^{\pm}\right)(t). \tag{3.16}$$

These series converge uniformly in each compact time interval to regular functions. Multiplying both members in this equality by t and using the general rule for causal convolutions,

$$t\frac{\overbrace{(f * \ldots * f)}^{k \text{ functions}}}{k!} = (tf) * \frac{\overbrace{(f * \ldots * f)}^{k-1 \text{ functions}}}{(k-1)!},$$

give the dyadic Volterra integral equations of the second kind

$$t\mathbf{P}^{\pm}(z;t) = -\mathbf{F}^{\pm}(t) - \big(\mathbf{F}^{\pm}(\cdot) * \mathbf{P}^{\pm}(z;\cdot)\big)(t), \;\; \mathbf{F}^{\pm}(t) = zt\mathbf{K}^{\pm}(t). \tag{3.17}$$

Now consider a concentrated source distributed over the plane $z = 0$:

$$\boldsymbol{J}^e_T(z,t) = \boldsymbol{j}^e(t)\delta(z).$$

The wave splitting shows that this current density generates the electric field

$$\boldsymbol{E}(0,t) = \boldsymbol{E}^{+}(+0,t) = \boldsymbol{E}^{-}(-0,t) = -\left(\mathbf{Z} * \boldsymbol{j}^e\right)(t)\eta/2$$

in the plane $z = 0$. Using these identities, equation (3.13) can be written as

$$\boldsymbol{E}^{\pm}(z,t) = \int \mathcal{E}^{\pm}(z;t-t') \cdot \boldsymbol{E}(0,t')\, dt' \tag{3.18}$$

or

$$\boldsymbol{E}^{\pm}(\pm z, t+z/c) = H(z)\mathbf{Q}^{\pm}(z) \cdot \left(\boldsymbol{E}(0,t) + \int_{-\infty}^{t} \mathbf{P}^{\pm}(z;t-t') \cdot \boldsymbol{E}(0,t')\, dt' \right).$$

Another way to put this is

$$\mathcal{E}^{\pm}(\pm z, t+z/c) = H(z) \left[\mathcal{P}^{\pm}(z)\delta \right](t), \tag{3.19}$$

where temporal integral operators

$$\mathcal{P}^{\pm}(z) = \mathbf{Q}^{\pm}(z) \cdot \left(\mathbf{I}_T \delta(\cdot) + \mathbf{P}^{\pm}(z;\cdot) \right) *$$

are the wave propagators for up- and down-going fields, respectively. These operators propagate the fields a distance z through the bi-gyrotropic medium. Obviously, the wave propagators can be written in the form

$$\mathcal{P}^{\pm}(z) = \mathbf{I}_T \mathcal{P}^{\pm}_{\text{co}}(z) + \mathbf{J}_T \mathcal{P}^{\pm}_{\text{cross}}(z),$$

where the operators $\mathcal{P}^{\pm}_{\text{co}}(z)$ and $\mathcal{P}^{\pm}_{\text{cross}}(z)$ are scalar. In operator sense,

$$\mathcal{P}^{\pm}(z) = \exp\left(-\frac{z}{c} \partial_t \left(\mathbf{I}_T N^{\pm}_{\text{co}} + \mathbf{J}_T N^{\pm}_{\text{cross}} \right) * \right). \tag{3.20}$$

Wave propagators are useful in the analysis of normal-incidence problems for isotropic and bi-isotropic half-spaces and slabs [11, 24], and it is conjectured that this is the case for bi-gyrotropic half-spaces and slabs as well.

The propagators, $\mathcal{P}^{+}(z)$, $-\infty < z < \infty$, form a group under multiplication and so do the propagators, $\mathcal{P}^{-}(z)$, $-\infty < z < \infty$:

$$\begin{cases} \mathcal{P}^{\pm}(z_1 + z_2) = \mathcal{P}^{\pm}(z_1) \cdot \mathcal{P}^{\pm}(z_2), \\ \mathcal{P}^{\pm}(0) = \mathbf{I}_T, \\ \left(\mathcal{P}^{\pm}\right)^{-1}(z) = \mathcal{P}^{\pm}(-z), \end{cases} \tag{3.21}$$

Observe that a positive wave-propagator argument, z, corresponds to propagation of up- or down-going waves a distance z through the bi-gyrotropic medium. A negative argument, $-z$, indicates that the inverse (resolvent operator) of the operator $\mathcal{P}^{\pm}(z)$ is referred to. Negative propagator arguments arise at signal restoration. The first propagator rule (3.21) is used below at numerical evaluations.

4 Complex time-dependent EM fields

In this section, complex time-dependent electromagnetic field vectors are introduced. The complex field-vector concept is well-known for isotropic and bi-isotropic materials [1, 18, 29] but seems to be new for general bi-gyrotropic media. The use of complex field vectors simplifies the analysis in Section 3. Specifically, vector and dyadic differential and integral equations for real-valued quantities reduce to scalar differential and integral equations for complex-valued functions. The obtained scalar equations are economical both theoretically and numerically. The electric field $\boldsymbol{E}_T(z,t)$, the magnetic field $\boldsymbol{H}_T(z,t)$, and the split vector fields $\boldsymbol{E}^{\pm}(z,t)$ can be replaced by the scalar, complex fields $E_c(t)$, $H_c(t)$, and $E_c^{\pm}(z,t)$, respectively. Similarly, the intrinsic dyadic integral kernels $\mathbf{N}^{\pm}(t)$, $\mathbf{Y}^{\pm}(t)$, and $\mathbf{Z}(t)$, and the dyadic propagator kernels $\mathbf{P}^{\pm}(z,t)$ can be replaced by scalar, complex kernels denoted by $N_c^{\pm}(t)$, $Y_c^{\pm}(t)$, $Z_c(t)$, and $P_c^{\pm}(z,t)$, respectively. Combining the complex field-vector and the wave-splitting concepts gives the problem an appropriate structure. Roughly speaking, the electromagnetic field is decomposed into four constituents: right-hand circularly polarized and left-hand circularly polarized up- and down-going fields.

Complex, time-dependent electromagnetic fields can be defined by introducing the projection dyadic

$$\mathbf{p} = \frac{1}{2}(\mathbf{I}_T - j\mathbf{J}_T),$$

where j is the imaginary unit. Let $\boldsymbol{F}_T(z,t)$ be an arbitrary (real) transverse field vector of the form (2.5). Operating on $\boldsymbol{F}_T$ with $\mathbf{p}$ gives the complex field

$$\boldsymbol{F}_c(z,t) = \mathbf{p}\cdot\boldsymbol{F}_T(z,t) = \frac{1}{2}(\boldsymbol{u}_x - j\boldsymbol{u}_y)F_c(z,t),$$

where the amplitude is $F_c(z,t) = F_x(z,t)+jF_y(z,t)$. The components of the physical field can be as

$$F_x(z,t) = \mathrm{Re}F_c(z,t), \qquad F_y(z,t) = \mathrm{Im}F_c(z,t).$$

Observe that the physical field can be written in the form $\boldsymbol{F}_T = \boldsymbol{F}_c + \boldsymbol{F}_c^*$, where the complex field vectors can be interpreted in terms well known from the time-harmonic analysis: $\boldsymbol{F}_c$ represents the RCP (LCP) component of $\boldsymbol{F}_T$ and $\boldsymbol{F}_c^*$ the LCP (RCP) component of $\boldsymbol{F}_T$ provided $\boldsymbol{F}_T$ is up-going (down-going).

Suppose now that $\mathbf{F}(t)$ is a (real) dyadic function of the form (3.4). Applying the projection operator on $\mathbf{F}$ gives

$$\mathbf{p}\cdot\mathbf{F} = \mathbf{p}\,(\delta + F_{\mathrm{co}} + jF_{\mathrm{cross}}) = \mathbf{p}\,(\delta + F_c)\,,$$

where the scalar $F_c(t) = F_{\mathrm{co}}(t)+jF_{\mathrm{cross}}(t)$ is complex. The co- and cross-components of the physical dyadic are obtained as

$$F_{\mathrm{co}}(t) = \mathrm{Re}F_c(t), \qquad F_{\mathrm{cross}}(t) = \mathrm{Im}F_c(t).$$

The above results can be applied to the differential and integral equations in Section 3. Multiplying both sides of equation (3.7) by $\mathbf{p}$ gives the scalar, first-order, dispersive wave equations

$$\partial_z E_c^{\pm} = \mp c^{-1}\partial_t \left(E_c^{\pm} + N_c^{\pm} * E_c^{\pm}\right) \mp \eta J_c^e/2 \mp (Z_c * \eta J_c^e)/2$$

for the complex split vector fields. Similarly, the refractive equations (3.9) become

$$\begin{aligned} 2N_c^{\pm} + N_c^{\pm} * N_c^{\pm} \mp jN_c^{\pm} * (\chi_c^{em} - \chi_c^{me}) \mp j\,(\chi_c^{em} - \chi_c^{me}) + \chi_c^{em} * \chi_c^{me} \\ = \chi_c^{ee} + \chi_c^{mm} + \chi_c^{ee} * \chi_c^{mm}, \end{aligned} \tag{4.1}$$

whereas the integral equations for the relative admittances (3.8) reduce to

$$N_c^{\pm}(t) = \chi_c^{mm}(t) + Y_c^{\mp}(t) + (\chi_c^{mm} * Y_c^{\mp})(t) \pm j\chi_c^{em}(t).$$

In terms of the complex admittances $Y_c^{\pm}(t)$ and the complex split field vectors $E_c^{\pm}(z,t)$, the complex electric and magnetic fields are

$$\begin{aligned} E_c &= E_c^{+} + E_c^{-}, \\ \eta H_c &= j(1 + Y_c^{+}*)E_c^{+} - j(1 + Y_c^{-}*)E_c^{-}. \end{aligned}$$

The wave propagator (3.20) can be represented by a complex wave propagator of the form $\mathcal{P}_c^{\pm}(z) = \mathcal{P}_{\rm co}^{\pm}(z) + j\mathcal{P}_{\rm cross}^{\pm}(z)$ given by

$$\mathcal{P}_c^{\pm}(z) = \exp\left(-\frac{z}{c}\partial_t N_c^{\pm}*\right) = Q_c^{\pm}(z)\big(1 + P_c^{\pm}(z;\cdot) * \big), \tag{4.2}$$

where the complex wave-front factors are

$$Q_c^{\pm}(z) = \exp\big(-N_c^{\pm}(+0)z/c\big). \tag{4.3}$$

The complex versions of the integro-differential equations (3.15) and the integral equations (3.17) are, respectively,

$$\partial_z P_c^{\pm}(z;t) = -K_c^{\pm}(t) - \big(K_c^{\pm}(\cdot) * P_c^{\pm}(z;\cdot)\big)(t), \quad P_c^{\pm}(0;t) = 0, \tag{4.4}$$

$$tP_c^{\pm}(z;t) = -F_c^{\pm}(t) - \big(F_c^{\pm}(\cdot) * P_c^{\pm}(z;\cdot)\big)\,(t), \quad F_c^{\pm}(t) = ztK_c^{\pm}(t), \tag{4.5}$$

where $K_c^{\pm}(t) = c^{-1}\left\{\partial_t N_c^{\pm}(t)\right\}$.

In the proceeding sections, the response to a concentrated source distributed over the plane $z = 0$ is considered. The integral representations (3.18) reduce to

$$E_c^{\pm}(z,t) = \int \mathcal{E}_c^{\pm}(z;t-t')E_c(0,t')\,dt',$$

where the complex fundamental solutions

$$\mathcal{E}_c^{\pm}(\pm z;t+z/c) = H(z)\left[\mathcal{P}_c^{\pm}(z)\delta\right](t) = H(z)Q_c^{\pm}(z)\big(\delta(t) + P_c^{\pm}(z;t)\big)$$

have been introduced via the identity $\mathbf{p}\cdot\mathcal{E}^{\pm}(z;t) = \mathbf{p}\mathcal{E}_c^{\pm}(z;t)$ and $E_c(0,t)$ is the complex electric field at $z = 0$. Specifically, the electric response $\mathcal{E}_x(z;t)$ to the x-polarized electric field $\boldsymbol{u}_x\delta(t)$ at $z = 0$ is in focus:

$$\mathcal{E}_x(\pm z;t+z/c) = \boldsymbol{u}_x\left[\mathcal{P}_{\rm co}^{\pm}(z)\delta\right](t) + \boldsymbol{u}_y\left[\mathcal{P}_{\rm cross}^{\pm}(z)\delta\right](t), \quad z > 0. \tag{4.6}$$

Obviously, it suffices to study the complex impulse response

$$\left[\mathcal{P}_{\rm co}^{\pm}(z)\delta\right](t) + j\left[\mathcal{P}_{\rm cross}^{\pm}(z)\delta\right](t) \equiv \left[\mathcal{P}_c^{\pm}(z)\delta\right](t) = Q_c^{\pm}(z)\big(\delta(t) + P_c^{\pm}(z;t)\big). \tag{4.7}$$

5 Forerunners in bi-gyrotropic media

In this section, the time-domain theory of forerunners in isotropic dielectrics presented in Ref. 11 is generalized to bi-gyrotropic materials.

Sommerfeld's forerunner is the short-time or leading-edge approximation to the impulse response given by equations (4.6)–(4.7). Straightforward generalization of the derivation in Ref. 11 gives the following expressions for the complex forerunners for up- and down-going waves, respectively:

$$\left[\mathcal{P}^{\pm}_{S,c}(z)\delta\right](t) = Q^{\pm}_c(z)\big(\delta(t) + P^{\pm}_{S,c}(z;t)\big), \tag{5.1}$$

where $Q^{\pm}_c(z)$ are the wave-front factors (4.3) and

$$P^{\pm}_{S,c}(z;t) = -zK^{\pm}_c(+0)\left(J_0\left(2\sqrt{zK^{\pm}_c(+0)t}\right) + J_2\left(2\sqrt{zK^{\pm}_c(+0)t}\right)\right)H(t). \tag{5.2}$$

Here $J_\nu(x)$ is the Bessel function of order ν. Observe that the arguments of the exponential and Bessel functions are complex in general and that the forerunners depend on the initial values $N^{\pm}_c(+0)$ and $K^{\pm}_c(+0)$ only. Naturally, Sommerfeld's forerunner can be obtained for other excitations by temporal convolution of the incident field and the right-hand side of (5.1).

The slowly varying components of the impulse response (4.6)–(4.7) constitute Brillouin's forerunner [11]. These components can be obtained by integrating the convolution terms in the first-order wave equations (4.4) repeatedly by parts, which results in a series of integrated terms. Truncating this series after one step gives a nondispersive, hyperbolic equation characterized by a wave-front speed less than c. Truncating the series after more then one step results in parabolic equations which are noncausal [12]. Once Brillouin's forerunner for the impulse response is known, straightforward temporal convolution gives the second forerunner for an arbitrary excitation.

An outline of the time-domain method of obtaining Brillouin's forerunner in the bi-gyrotropic medium is now given. As in Ref. 11, the exponential representation (4.2) of the complex wave propagator is expanded with respect to slowly varying fields. The first step is to expand the convolution operators χ_c* and $N^{\pm}_c*$ as

$$\chi_c* = \sum_{i=1}^{s} \chi_i \frac{d^{i-1}}{dt^{i-1}} + R_{\chi,s}* \frac{d^s}{dt^s}, \qquad N^{\pm}_c* = \sum_{i=1}^{s} n^{\pm}_i \frac{d^{i-1}}{dt^{i-1}} + R^{\pm}_{n,s}* \frac{d^s}{dt^s}, \tag{5.3}$$

where $\chi_c(t) = \chi^{kl}_c(t)$, $k,l = e,m$. These expansions correspond to the integrations by parts discussed in the previous paragraph. The complex coefficients χ_i, $i = 1,2,\cdots,s$ are proportional to the moments of $\chi_c(t)$,

$$\chi_i = \frac{(-1)^{i-1}}{(i-1)!}\int_0^\infty t^{i-1}\chi_c(t)\,dt,$$

and the remainder, $R_{\chi,s}(t)$, is given by

$$R_{\chi,s}(t) = \frac{(-1)^s}{(s-1)!}\left(\int_t^\infty (\tau - t)^{s-1}\chi_c(\tau)\,d\tau\right)H(t).$$

The quantities $n_i^{\pm}$ and $R_{n,s}^{\pm}(t)$ are defined analogously. To proceed, suppose that χ_i and $n_i^{\pm}$ are finite and that $R_{\chi,s}$, $R_{n,s}^{\pm}$ tend to zero as s goes to infinity. Given the susceptibility coefficients χ_i, one can calculate the refractive coefficients $n_i^{\pm}$ using the recurrence formulae

$$2n_{m+1}^{\pm}+\sum_{i=0}^{m} n_{m-i+1}^{\pm}n_{i+1}^{\pm}\pm j\sum_{i=0}^{m} n_{m-i+1}^{\pm}(\chi_{i+1}^{me}-\chi_{i+1}^{em})\pm j(\chi_{m+1}^{me}-\chi_{m+1}^{em})+\sum_{i=0}^{m}\chi_{m-i+1}^{em}\chi_{i+1}^{me}$$
$$=\chi_{m+1}^{ee}+\chi_{m+1}^{mm}+\sum_{i=0}^{m}\chi_{m-i+1}^{ee}\chi_{i+1}^{mm}. \tag{5.4}$$

These relations follow immediately from the integral equations (4.1) and the operator expansions (5.3).

Since down-going waves can be treated analogously, it suffices to continue the discussion for up-going fields only. The superscripts $\pm$ can, therefore, be dropped. The general time-dependence is suppressed as well.

Using the expansions of the refractive operators (5.3), the expression (4.2) for the complex wave propagator for up-going waves, $\mathcal{P}_c(z)$, can be written formally as

$$\mathcal{P}_c(z)=\exp\left\{-\frac{z}{c}\frac{d}{dt}\sum_{i=1}^{s} n_i\frac{d^{(i-1)}}{dt^{(i-1)}}\right\}\mathcal{P}_{s+1}(z), \tag{5.5}$$

where

$$\mathcal{P}_{s+1}(z)=\exp\left\{-\frac{z}{c}\frac{d}{dt}R_{n,s}*\frac{d^s}{dt^s}\right\}.$$

An approximation to $\mathcal{P}_c(z)$ can be obtained by keeping an appropriate even number m of terms in the expansion (5.5):

$$\mathcal{P}_c(z)\approx\exp\left\{-\frac{z}{c}\frac{d}{dt}\sum_{i=1}^{m} n_i\frac{d^{(i-1)}}{dt^{(i-1)}}\right\}=:T_m(z;\cdot)* \tag{5.6}$$

This approximation is a convolution operator with a smooth (analytic) kernel $T_m(z;t)$ given by the inverse Fourier-transform. Specifically,

$$T_m(z;t)=\frac{1}{2\pi}\int_{-\infty}^{\infty}\exp\left\{jwt-\frac{z}{c}\left(n_1jw+n_2(jw)^2+\cdots+n_m(jw)^m\right)\right\}dw$$
$$=\frac{1}{2\pi}\int_{-\infty}^{\infty}\exp\left\{jwt-\frac{z}{c}\left(n_1^{(1)}jw+n_2^{(1)}(jw)^2+\cdots+n_{m-2}^{(1)}(jw)^{m-2}\right)\right\}dw$$
$$*\exp\left\{\frac{z}{c}n_m\left(\frac{n_{m-1}}{mn_m}\right)^m\right\}\frac{1}{2\pi}\int_{-\infty}^{\infty}\exp\left\{jwt-\frac{z}{c}n_m\left(jw+\frac{n_{m-1}}{mn_m}\right)^m\right\}dw,$$

where the introduced coefficients are

$$n_i^{(1)}=n_i-n_m\binom{m}{i}\left(\frac{n_{m-1}}{mn_m}\right)^{m-i}.$$

Assuming that $(-1)^{m/2}\mathrm{Re}n_m > 0$, the last integral in this expression can be recognized as a hyper-Airy function of even order m and complex argument, $\mathrm{A}_m(x)$; see Appendix A; consequently,

$$\begin{aligned} T_m(z;t) =& \frac{1}{2\pi}\int_{-\infty}^{\infty} \exp\left\{jwt - \frac{z}{c}\left((n_1^{(1)}jw + n_2^{(1)}(jw)^2 + \cdots + n_{m-2}^{(1)}(jw)^{m-2}\right)\right\} dw \\ & * \exp\left\{\frac{z}{c}n_m\left(\frac{n_{m-1}}{mn_m}\right)^m - t\frac{n_{m-1}}{mn_m}\right\}\frac{1}{t_m}\,\mathrm{A}_m\left(\frac{t}{t_m}\right), \end{aligned}$$

where the analyticity of the integrand has been exploited and the complex scaling time is given by

$$t_m = \left((-1)^{m/2}\frac{zmn_m}{c}\right)^{1/m}.$$

If $(-1)^{(m-2)/2}\mathrm{Re}n_{m-2} > 0$, the integral to the left of the convolution star can be treated analogously. Assuming that

$$(-1)^{\frac{i}{2}}\mathrm{Re}n_i^{(\frac{m-i}{2})} > 0, \qquad i = 2, 4, \cdots, m \tag{5.7}$$

and progressing in the way described above, one obtains an expression for the kernel $T_m(z;t)$ in terms of a convolution of $\frac{m}{2}$ functions. Each of these is a product of a hyper-Airy function of even order and an exponential function and is therefore smooth. Explicitly,

$$\mathcal{P}_c \approx P_2 * P_4 * \cdots * P_m *, \tag{5.8}$$

where

$$\begin{cases} P_i(z;t) = \exp\left\{\dfrac{z}{c}n_i^{(\frac{m-i}{2})}\left(\dfrac{n_{i-1}^{(\frac{m-i}{2})}}{in_i^{(\frac{m-i}{2})}}\right)^i - t\left(\dfrac{n_{i-1}^{(\frac{m-i}{2})}}{in_i^{(\frac{m-i}{2})}}\right)\right\}\dfrac{1}{t_i}\,\mathrm{A}_i\left(\dfrac{t}{t_i}\right), \\ t_i = \left((-1)^{i/2}\dfrac{zin_i^{(\frac{m-i}{2})}}{c}\right)^{1/i} \end{cases} \tag{5.9}$$

for $i = 2, 4, \cdots, m$. Here, the refractive coefficients are

$$\begin{cases} n_i^{(0)} = n_i, \\ n_i^{(\frac{m-i}{2})} = n_i - \displaystyle\sum_{l=\frac{i}{2}+1}^{\frac{m}{2}} n_{2l}\binom{2l}{i}\left(\frac{n_{2l-1}}{2ln_{2l}}\right)^{2l-i}, \\ n_{i-1}^{(\frac{m-i}{2})} = n_{i-1} - \displaystyle\sum_{l=\frac{i}{2}+1}^{\frac{m}{2}} n_{2l}\binom{2l}{i-1}\left(\frac{n_{2l-1}}{2ln_{2l}}\right)^{2l-i+1}. \end{cases}$$

Now we are able to formulate the condition on m in (5.6): m has to be chosen so that the assumption (5.7) is fulfilled. This is the case in the examples described in Sections 6 and 7.

A closed-form approximation to the second forerunner can be obtained in the special case $m = 2$:

$$\begin{cases} \mathcal{P}_c(z) \approx P_2(z,\cdot)*, \\ P_2(z;t) = \dfrac{1}{t_2} A_2\left(\dfrac{t-t_1}{t_2}\right) = \dfrac{1}{\sqrt{2\pi}\, t_2} \exp\left\{-\dfrac{(t-t_1)^2}{2t_2^2}\right\}, \\ t_1 = \dfrac{n_1 z}{c}, \qquad t_2 = \sqrt{-\dfrac{2zn_2}{c}}, \end{cases} \tag{5.10}$$

where the refractive coefficients n_1 and n_2 can be calculated from the recurrence formula (5.4). This crude approximation has the right order of amplitude, some of the dynamics of the actual propagator kernel (see Figures 1, 2, 4, and 5), and is easy to generate.

For an isotropic chiral medium, the noncausal approximation $P_2(z; t - z/c)$ can be compared to the complex propagator kernel $\frac{1}{t_g} A_2(\frac{t - z\sqrt{\mu\epsilon}}{t_g})$, $t_g = \sqrt{2jgz}$ associated with Condon's model, $\boldsymbol{D} = \epsilon \boldsymbol{E} - g\partial_t \boldsymbol{H}$, $\boldsymbol{B} = \mu \boldsymbol{H} + g\partial_t \boldsymbol{E}$, where $\epsilon > 0$, $\mu > 0$, and g are real numbers modeling permittivity, permeability, and chirality, respectively [5, 7]. Thus, Condon's model can be interpreted as a first-order nondispersive approximation to the dynamics of charges in a bi-isotropic medium.

It should also be mentioned that a better approximation than (5.10) to the operator $\mathcal{P}_c(z)$ can be obtained in a closed form, even though slightly different technique is used to derive it. Using (5.6) with $m = 3$ gives

$$\begin{aligned} \mathcal{P}_c(z) \approx P_B(z;\cdot)* &= \exp\left(-\frac{z}{c}\partial_t(n_1 + n_2\partial_t + n_3\partial_t^2)\right) \\ &= \exp\left(-\frac{z}{c}\left(n_3\left(\partial_t + \frac{n_2}{3n_3}\right)^3 + \left(n_1 - \frac{n_2^2}{3n_3}\right)\partial_t - \frac{n_2^3}{27n_3^2}\right)\right). \end{aligned}$$

The kernel $P_B(z;t)$ satisfies, cf. (4.4),

$$-c\partial_z P_B(z;t) = (n_1\partial_t + n_2\partial_t^2 + n_3\partial_t^3)P_B(z;t), \qquad P_B(0+;t) = \delta(t).$$

Generalization of the result in Karlsson and Rikte [11] gives

$$P_B(z;t) = \exp\left(\frac{n_2^3}{27n_3^2}\frac{z}{c} - \frac{n_2}{3n_3}(t - t_1(z))\frac{Ai(\mathrm{sign}(\mathrm{Re}(n_3))(t - t_1(z))/t_3(z))}{t_3(z)}\right),$$

where

$$t_1(z) = \left(n_1 - \frac{n_2^2}{3n_3}\right)\frac{z}{c}, \qquad t_3(z) = \left(\frac{3n_3\mathrm{sign}(\mathrm{Re}(n_3))z}{c}\right)^{1/3}.$$

This approximation is a generalization of the classical result obtained by Brillouin for single-resonance Lorentz materials [3, 4]. The formula above can be verified by direct differentiation.

6 Examples

In this section, two theoretical examples are given. Numerical results are presented in Section 7.

6.1 A bi-isotropic single-resonance medium

6.1.1 Physical background

In this subsection, a time-domain derivation of Drude's molecular model for reciprocal, nonmagnetic, isotropic chiral materials is presented.

Post's constitutive relations are often used to model optical activity:

$$\begin{cases} c\eta \boldsymbol{D}(\boldsymbol{r},t) = \boldsymbol{E}(\boldsymbol{r},t) + \big(\chi_P^{ee} * \boldsymbol{E}\big)(\boldsymbol{r},t) + c\big(\chi_P^{em} * \boldsymbol{B}\big)(\boldsymbol{r},t), \\ \eta \boldsymbol{H}(\boldsymbol{r},t) = \big(\chi_P^{me} * \boldsymbol{E}\big)(\boldsymbol{r},t) + c\boldsymbol{B}(\boldsymbol{r},t) + c\big(\chi_P^{mm} * \boldsymbol{B}\big)(\boldsymbol{r},t), \end{cases} \tag{6.1}$$

These constitutive relations are equivalent to (2.1) and the connection between these is given by a system of Volterra integral equations of the second kind [14].

For reciprocal, nonmagnetic, isotropic chiral materials, $\chi_P^{ee}(t) = G(t)$, $\chi_P^{em}(t) = \chi_P^{me}(t) = \kappa(t)$, and $\chi_P^{mm}(t) = 0$. Denoting the electron density by N, the electric polarization can be written in the form

$$Nq\boldsymbol{r}(t) = \epsilon_0 (G * \boldsymbol{E})(t) + \epsilon_0 (\kappa * c\boldsymbol{B})(t), \tag{6.2}$$

where $\boldsymbol{r}(t)$ is the displacement of an electron relative to its position of equilibrium, $q = -e$ is the charge of the electron, and $\epsilon_0 = 1/(c\eta)$ the permittivity of vacuum. For an electron in helical motion, the equation for $\boldsymbol{r}(t)$ becomes

$$m\partial_t^2 \boldsymbol{r}(t) = -m\nu\partial_t \boldsymbol{r}(t) - m\omega_0^2 \boldsymbol{r}(t) + q\boldsymbol{E}(t) - qc\alpha \nabla \times \boldsymbol{E},$$

where m is the mass of the electron at rest, $\nu \geq 0$ the collision frequency, $\omega_0 \geq 0$ the natural (harmonic) frequency, and α a positive or negative constant depending on the micro-structure of the chiral medium.

Substituting the polarization, (6.2), and Faraday's law, $\nabla \times \boldsymbol{E} = -\partial_t \boldsymbol{B}$, into this equation gives

$$\big(\partial_t^2 + \nu\partial_t + \omega_0^2\big)\big((G * \boldsymbol{E})(t) + (\kappa * c\boldsymbol{B})(t)\big) = \omega_p^2\big(\boldsymbol{E}(t) + \alpha\partial_t c\boldsymbol{B}(t)\big).$$

Setting $\boldsymbol{B} = \boldsymbol{0}$ shows that the electric susceptibility kernel is given by Lorentz' dispersion model; setting $\boldsymbol{E} = \boldsymbol{0}$, shows that the chirality kernel is proportional to the time-derivative of the electric susceptibility kernel; consequently,

$$G(t) = H(t)\frac{\omega_p^2}{\nu_0}\sin(\nu_0 t)\exp\left(-\frac{\nu t}{2}\right), \qquad \kappa(t) = \alpha\partial_t G(t), \tag{6.3}$$

where $\omega_p = \sqrt{Nq^2/(\epsilon_0 m)}$ and $\nu_0 = \sqrt{\omega_0^2 - \nu^2/4}$. This model was obtained first by Drude [6] but is often referred to as Condon's model [5]. For passive materials, $|\alpha|$ is subjected to an upper bound which depends on ω_0, ω_p, and ν [16].

6.1.2 Forerunners

In terms of the constitutive relations (2.1), the results in the previous subsection can be written as

$$\begin{cases} \chi_{\rm co}^{em}(t) = -\chi_{\rm co}^{me}(t) = \kappa(t) = \alpha\partial_t G(t), \\ \chi_{\rm co}^{ee}(t) = \chi(t) = G(t) - (\kappa * \kappa)(t), \\ \chi_{\rm cross}^{em}(t) = \chi_{\rm cross}^{me} = \chi_{\rm cross}^{ee} = \chi_{\rm co}^{mm} = \chi_{\rm cross}^{mm} = 0, \end{cases} \tag{6.4}$$

where $G(t)$ is given by equation (6.3). The refractive equation (3.9) now reduces to

$$(N_{\rm co} * N_{\rm co})(t) + 2N_{\rm co}(t) = \chi(t), \qquad N_{\rm cross}(t) = \kappa(t).$$

Sommerfeld's forerunner for this chiral medium is given by equations (5.1)–(5.2), where $N_c(+0) = j\alpha\omega_p^2$ and $K_c(+0) = (\omega_p^2(1-\alpha^2\omega_p^2)/2 - j\alpha\nu\omega_p^2)/c$.

To obtain Brillouin's forerunner, expand the operators $G*$ and $\kappa*$ according to (5.3), $m \geq 1$:

$$\begin{cases} g_m = \dfrac{(-1)^{m-1}}{(m-1)!}\displaystyle\int_0^\infty t^{m-1}G(t)\,dt = (-1)^{m+1}\frac{\omega_p^2}{\omega_0^m\nu_0}\sin\left(m\arcsin\left(\frac{\nu_0}{\omega_0}\right)\right), \\ \kappa_1 = 0, \qquad \kappa_{m+1} = \alpha g_m, \\ \chi_m = g_m - \displaystyle\sum_{i=1}^{m-2}\kappa_{i+1}\kappa_{m-i}. \end{cases}$$

The recurrence formula (5.4) gives

$$\begin{cases} n_1 = \sqrt{1+\chi_1} - 1, \\ {\rm Re}n_{m+1} = \dfrac{\chi_{m+1} - \sum_{i=1}^{m-1}{\rm Re}n_{m-i+1}{\rm Re}n_{i+1}}{2(1+n_1)}, \qquad {\rm Im}n_{m+1} = \kappa_{m+1}. \end{cases}$$

Explicitly, the first coefficients are:

$$\begin{cases} \chi_1 = \dfrac{\omega_p^2}{\omega_0^2}, \qquad \chi_2 = -\dfrac{\nu\omega_p^2}{\omega_0^4}, \\ n_1 = \sqrt{1+\omega_p^2/\omega_0^2} - 1, \qquad n_2 = -\dfrac{1}{\sqrt{1+\omega_p^2/\omega_0^2}}\dfrac{\nu\omega_p^2}{2\omega_0^4} + j\dfrac{\alpha w_p^2}{w_0^2}, \end{cases}$$

Notice that $\mathbb{R} \ni n_1 > 0$, ${\rm Re}n_2 < 0$. The coefficients n_k, $k > 2$ are obtained from the recurrence relation above. The methods described in section 5 can now be used to calculate approximations to the second forerunner in the chiral medium. In the numerical example below, the condition (5.7) is fulfilled at least for $m = 6$.

6.2 A gyrotropic single-resonance medium

6.2.1 Physical background

Consider an electrically neutral, isotropic material subjected to a strong, constant external magnetic field, say $\boldsymbol{B}_0 = B_0\boldsymbol{u}_z$. Approximately, the polarization is of the

form $\epsilon_0(\boldsymbol{\chi}^{ee} * \boldsymbol{E})(t)$ and the magnetization zero, that is, the constitutive relations are given by $c\eta \boldsymbol{D} = \boldsymbol{E} + \boldsymbol{\chi}^{ee} * \boldsymbol{E}$ and $c\boldsymbol{B} = \eta \boldsymbol{H}$. A simple expression for the constitutive dyadic, $\boldsymbol{\chi}^{ee}(t)$, for this gyrotropic medium is now derived.

Assume the positive charges are heavy and let the electron density be N. The electric polarization can then be written in the form $\epsilon_0(\boldsymbol{\chi}^{ee} * \boldsymbol{E})(t) = Nq\boldsymbol{r}(t)$, where the time-dependent displacement vector, $\boldsymbol{r}(t)$, of an electron is determined by Newton's law of motion:

$$m\partial_t^2 \boldsymbol{r}(t) = -m\nu\partial_t \boldsymbol{r}(t) - m\omega_0^2 \boldsymbol{r}(t) + q\boldsymbol{E}(t) + q\partial_t \boldsymbol{r}(t) \times \boldsymbol{B}_0. \tag{6.5}$$

The first term in the right-hand side is a phenomenological damping force, the second term is a restoring Hooke's force, and the last two terms constitute a relevant approximation to the Lorentz force. The fourth term gives rise to the well-known Faraday effect, exhibited by the gyrotropic medium. The plasma frequency and the gyrotropic frequency are defined by $\omega_p = \sqrt{Nq^2/(\epsilon_0 m)}$ and $\omega_g = qB_0/m$, respectively. Newton's law of motion, (6.5), gives an ordinary differential equation for the polarization:

$$\left(\partial_t^2 + \nu\partial_t + \omega_0^2\right)(\boldsymbol{\chi}^{ee} * \boldsymbol{E})(t) + \omega_g \boldsymbol{u}_z \times \partial_t(\boldsymbol{\chi}^{ee} * \boldsymbol{E})(t) = \omega_p^2 \boldsymbol{E}(t).$$

Using that this equation holds for any electric field gives

$$\boldsymbol{\chi}^{ee}(t) = \mathbf{I}_T \chi_{\text{co}}^{ee}(t) + \mathbf{J}_T \chi_{\text{cross}}^{ee}(t) + \boldsymbol{u}_z \boldsymbol{u}_z \chi_z^{ee}(t), \tag{6.6}$$

where

$$\begin{cases} \chi_{\text{co}}^{ee}(t) = \text{Re}\chi_c^{ee}(t), \qquad \chi_{\text{cross}}^{ee}(t) = \text{Im}\chi_c^{ee}(t), \\ \chi_c^{ee}(t) = H(t)\dfrac{\omega_p^2}{\nu_{0c}} \sin(\nu_{0c}t) \exp\left(-\dfrac{\nu_c t}{2}\right), \\ \chi_z^{ee}(t) = H(t)\dfrac{\omega_p^2}{\nu_0} \sin(\nu_0 t) \exp\left(-\dfrac{\nu t}{2}\right), \end{cases} \tag{6.7}$$

and the introduced frequencies are

$$\nu_c = \nu + j\omega_g, \qquad \nu_{0c} = \sqrt{\omega_0^2 - \nu_c^2/4}, \quad \text{and} \quad \nu_0 = \sqrt{\omega_0^2 - \nu^2/4}.$$

The plasma is an example of a gyrotropic medium for which $\omega_0 = 0$.

6.2.2 Forerunners

For the gyrotropic medium discussed in the previous subsection, the refractive equation (4.1) reduces to

$$2N_c(t) + (N_c * N_c)(t) = \chi_c^{ee}(t).$$

Sommerfeld's forerunner is given by equations (5.1)–(5.2), where $N_c(+0) = 0$ and $K_c(+0) = \omega_p^2/(2c)$.

Brillouin's forerunner is now discussed. The moments of $\chi_c^{ee}(t)$ are

$$\chi_m^{ee} = \frac{(-1)^{m-1}}{(m-1)!}\int_0^\infty t^{m-1}\chi_c^{ee}(t)\,dt = (-1)^{m+1}\frac{\omega_p^2}{\omega_0^m\nu_{0c}}\sin\left(m\arcsin\left(\frac{\nu_{0c}}{\omega_0}\right)\right).$$

Explicitly, the first and second moments are $\chi_1^{ee} = \omega_p^2/\omega_0^2$ and $\chi_2^{ee} = -\nu_c\omega_p^2/\omega_0^4$. The corresponding refractive coefficients, n_m, are determined from the recurrence relation (5.4):

$$\begin{cases} n_1 = \sqrt{1+\chi_1^{ee}} - 1, \\ n_{m+1} = \dfrac{\chi_{m+1}^{ee} - \sum_{i=1}^{m-1} n_{m-i+1}n_{i+1}}{2(1+n_1)}, \qquad m \geq 1. \end{cases}$$

Specifically, the first and second refractive coefficients are $n_1 = \sqrt{1+\omega_p^2/\omega_0^2} - 1 > 0$ and $n_2 = -\nu_c\omega_p^2/(2\omega_0^4\sqrt{1+\omega_p^2/\omega_0^2}) < 0$. The methods described in Section 5 can now be used provided the condition (5.7) is fulfilled for some reasonable m. This is the case in the numerical example discussed below ($m = 10$).

7 Numerical calculations

The complex propagator kernel, $P_c(z;t)$, defined in Section 4, can be calculated numerically using different time-domain methods. One way is to solve the complex integro-differential equation (4.4) in a finite interval $[0,z]\times[0,t]$ using the method of characteristics. This is quite time consuming, since a convolution has to be performed at every step in the spatial variable z. For a fixed propagation depth, z, a more efficient way is to solve the Volterra integral equation of the second kind (4.5). The real-valued version of this integral equation was solved in Ref. 11. The complex-valued version is solved in a similar way. A third time-domain method of calculating $P_c(z;t)$ is to use the complex equivalent of the series expansion (3.16). It should be pointed out that the rule

$$P_c(z_1+z_2;t) = P_c(z_1;t) + P_c(z_2;t) + \left(P_c(z_1;\cdot) * P_c(z_2;\cdot)\right)(t), \tag{7.1}$$

can be utilized in the calculation of $P_c(z;t)$ in all three cases. This rule is due to the group properties (3.21). In fact, numerical tests indicate that it is necessary to use the rule (7.1) in order to obtain correct results for (comparatively) large propagation depths also for bi-gyrotropic materials.

Asymptotic expressions for the complex propagator kernel $Q_c(z)P_c(z;t)$ are obtained in Section 5 via repeated convolution (5.8). The functions P_{2k} can be expressed in terms of the hyper-Airy functions $A_{2k}(x)$, which are analyzed in Appendix A. For a small complex argument z, the hyper-Airy functions, $A_{2k}(z)$, can be obtained numerically by solving the ODEs (A.2) subjected to the initial conditions (A.3). Alternatively, the Volterra integral equations (A.4) or the Fourier

integrals (A.1) can be employed. Experience indicates that the asymptotic expressions (A.5) have to be used when the modulus of the argument, $|z|$, is larger than approximately 5.

The accuracy of the asymptotic expansions for the two material models presented in Section 6 is demonstrated in Figures 1, 2, 4, and 5. The forerunner approximations are compared to numerical results for the propagator kernel $Q_c(z)P_c(z;t)$, which are obtained by first solving the Volterra integral equation (4.5) at $z/2$, whereupon the propagator rule (7.1) is applied once. Due to the oscillatory behavior of the first precursor, a large number of data points is needed. In both cases, $32768 = 2^{15}$ data points are used.

Figures 1 and 2 illustrate the co- and cross-propagator kernels, respectively, for an isotropic chiral medium characterized by the parameters $\omega_p = \omega_0 = 100 \times c/z$, $\nu = 20 \times c/z$, and $\alpha = -0.001 \times z/c$, where z is the propagation depth. The polar plot of the co-propagator kernel versus the cross-propagator kernel with the time as parameter is presented in Figure 3. The second forerunner is clearly distinguishable as an irregularity in the spiral curve. For $z = 10^{-6}$ m, the values of parameters ω_p, ω_0, and α coincide with the ones used by Zablocky and Engheta [30]. In this reference, the medium was magnetic but lossless though ($\nu = 0$).

Figures 4 and 5 show the co- and cross-propagator kernels, respectively, for a gyrotropic medium characterized by the following parameters: $\omega_p = \omega_0 = \omega_g = 100 \times c/z$, and $\nu = 20 \times c/z$. The polar plot of the co-propagator kernel versus the cross-propagator kernel with the time as parameter is presented in Figure 6. The second forerunner is displayed in the more detailed Figure 6b.

In the second example, the method for obtaining the second forerunner described in Section 5 was modified in order to escape numerical problems arising at the calculation of the kernel P_4 as it stands in (5.9). To cope with this, the coefficient n_3 is separated into its real and imaginary parts. Taking $j\mathrm{Im}n_3$ as n_3, the method presented in Section 5 can be applied. To compensate for the real part of n_3, a convolution with the kernel

$$\begin{cases} P_3(z;t) = \dfrac{1}{t_3} Ai\left(-\dfrac{t}{t_3}\right), \\ t_3 = \left(\dfrac{3(-\mathrm{Re}n_3)z}{c}\right)^{\frac{1}{3}} \end{cases}$$

has to be performed, cf. Ref. 11.

The examples indicate that the difference between the numerical results for the complex propagator kernel $Q_c(z)P_c(z;t)$ and the asymptotic approximations decreases when the number of factors in the multiple convolution (5.8) increases. In particular, the tail of Brillouin's forerunner is improved significantly.

8 Conclusions

This paper concerns TEM pulse propagation along the gyrotropic axis in temporally dispersive bi-gyrotropic media. This class of linear, causal materials comprises 12

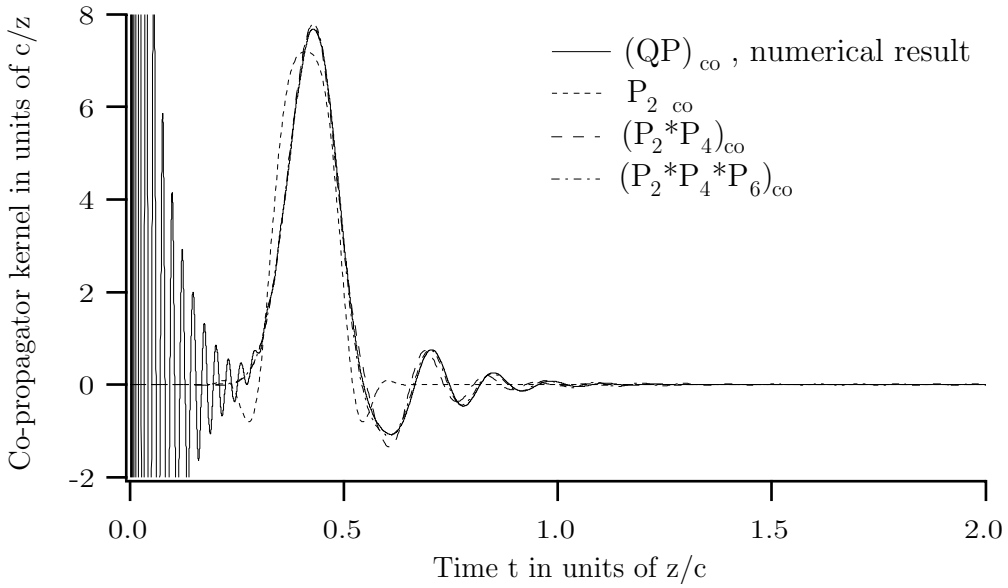

Figure 1: The co-propagator kernel, $(QP)_{\rm co}(z,t) = {\rm Re}\{Q_c(z)P_c(z;t)\}$, at a fixed propagation depth, z, in an isotropic chiral medium ($\omega_p = 100\times c/z$, $\omega_0 = 100\times c/z$, $\nu = 20\times c/z$, $\alpha = -0.001\times z/c$). 32768 data points were used at the equidistant discretization of the time interval $0 < t < 2\times z/c$. The leading-edge behavior is characterized by high amplitudes ($\approx 4000\times c/z$). Several second precursor approximations obtained by the time-domain method are shown also.

time-varying constitutive parameters, but only eight of these enter the problem discussed in this article. In particular, the impulse response and the first and second forerunners associated with this TEM pulse are investigated. Responses to other excitations can be obtained by temporal convolution.

The results are obtained employing time-domain techniques. Dispersive wave splitting is adopted to decompose the propagating waves into their up- and down-going constituents. Complex time-varying electromagnetic fields are used as well. Introducing this concept reduces relevant vector- and dyadic-valued equations for the up- and down-going field components to complex scalar equations that are easier to analyze and use for numerical purposes. Both dispersive wave splitting and complex fields have been used before in the analysis of the propagation of pulses in bi-isotropic media, but not simultaneously. The application to general bi-gyrotropic materials seems to be new as well. It should be observed that any physical field can be written as the sum of two complex conjugate, time-varying field vectors, which correspond to the RCP and LCP field components in the time-harmonic analysis.

The analysis shows that some features are common for all bi-gyrotropic media. First, these materials all support TEM waves along the gyrotropic axis. Second, they rotate propagating field vectors, although the physical mechanisms behind the rotations may be different (cf. Faraday effect and optical activity). Third, precursors generally arise in these materials. Otherwise, the behavior of propagating signals differs much from one bi-gyrotropic material to another. Figures 3 and 6 confirm

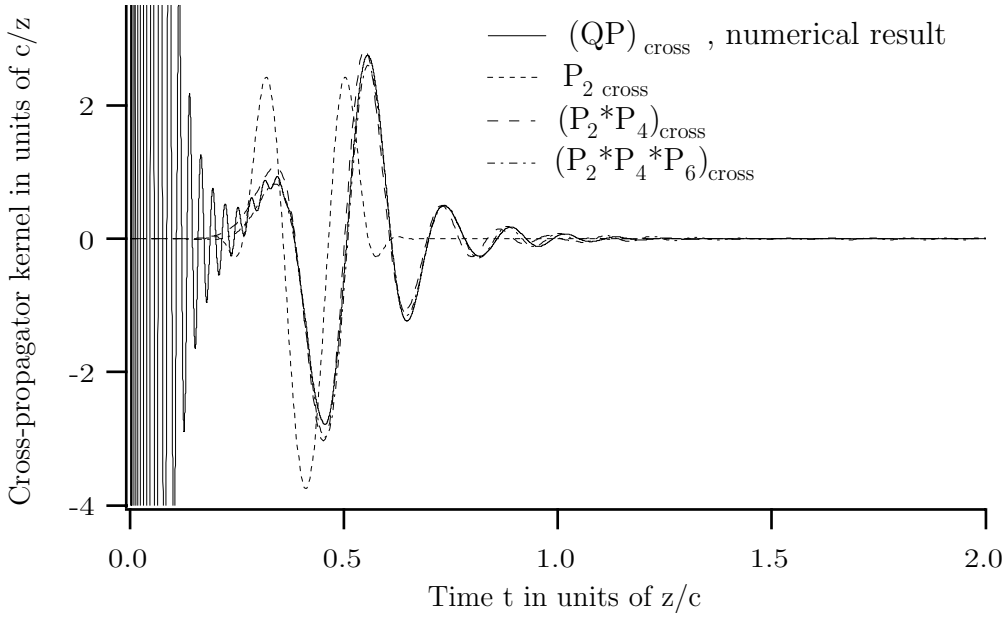

Figure 2: The cross-propagator kernel, $(QP)_{\text{cross}}(z,t) = \text{Im}\{Q_c(z)P_c(z;t)\}$, and second precursor approximations to this kernel at a fixed propagation depth, z, in an isotropic chiral medium. For parameters see caption of Figure 1. The leading-edge behavior of the numerical result is characterized by amplitudes of order $2500 \times c/z$.

this. The behavior in the general case is conjectured to be complicated.

The main purpose of the present work is the investigation of forerunners in bi-gyrotropic media in the vein of Ref. 11. Thus, endeavor to focus on the general aspects without going into details has guided the authors. The applied methods are general enough, although they are not claimed to work for all dispersion models. Examples indicate that single or multiple resonance type models seem appropriate to analyze using these techniques. The employed methods are simple from a mathematical point of view: no complicated asymptotic analysis of Fourier integrals is involved. A general advantage of time-domain techniques is that it is easier to find a physical meaning for time-varying than for frequency-dependent quantities. In particular, causality is maintained explicitly in each step until we come to discussion of the second precursor, where it is necessary to abandon it.

Using complex time-dependent field vectors, much of the theory of precursors in isotropic materials can be adopted [11]. The first precursor is the early time behavior of the propagating field and the second precursor the result of parabolic approximations to this field. The first forerunner can be expressed in terms of Bessel functions of complex arguments in analogy with the isotropic case. The theory of the second forerunner, however, must be modified. The final result involves convolutions of hyper-Airy functions of even orders and complex arguments. The obtained expression comprises half as many terms as the one presented in [11]. This makes it more attractive from the numerical point of view since convolution is a time- and memory-consuming operation. Brillouin's forerunners in two specific

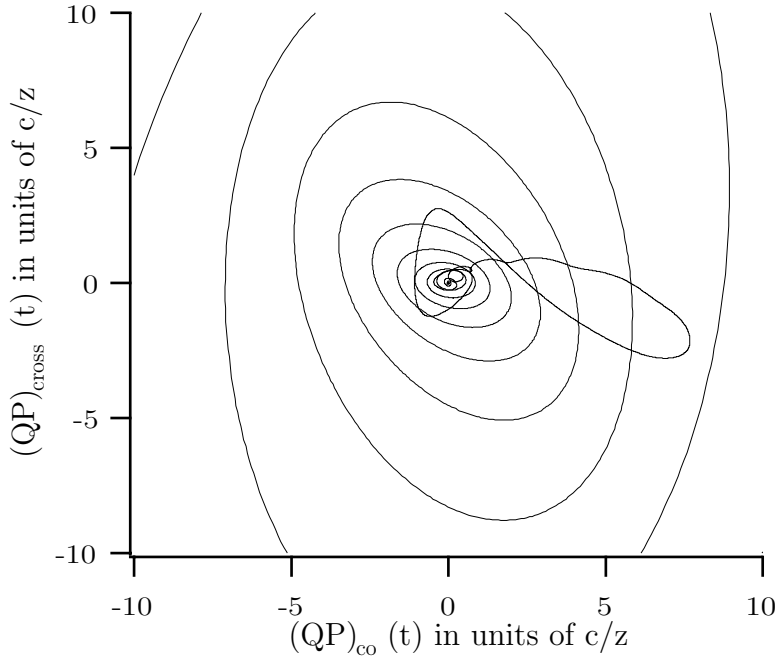

Figure 3: Polar plot of $(QP)_{\text{cross}}(z,t)$ versus $(QP)_{\text{co}}(z,t)$ with time as the parameter at a fixed propagation depth, z, in an isotropic chiral medium. The field is propagating towards the reader. Early times correspond to large amplitudes.

complex materials are investigated in some detail. Numerical calculations show good agreement between propagator kernels and forerunner approximations. In fact, even the lowest-order approximation to the second forerunner — a Gaussian of complex argument — contains much of the low-frequency behavior of the field.

A possible way to generalize the presented results is to analyze pulses that propagate in other directions than along the gyrotropic axis. More generally, access to the Green dyadics of the bi-gyrotropic medium makes it possible to obtain forerunners due to 3D source distributions using similar techniques.

Acknowledgments

The authors wish to thank Professor Ari Sihvola for reading through this manuscript and for giving valuable comments concerning the presentation of this work. In particular, the authors have benefited much from his excellent knowledge of the variety of bi-gyrotropic materials and the electromagnetic effects exhibited by these media.

The work reported in this paper is partially supported by a grant from the Swedish Research Council for Engineering Sciences, and its support is gratefully acknowledged.

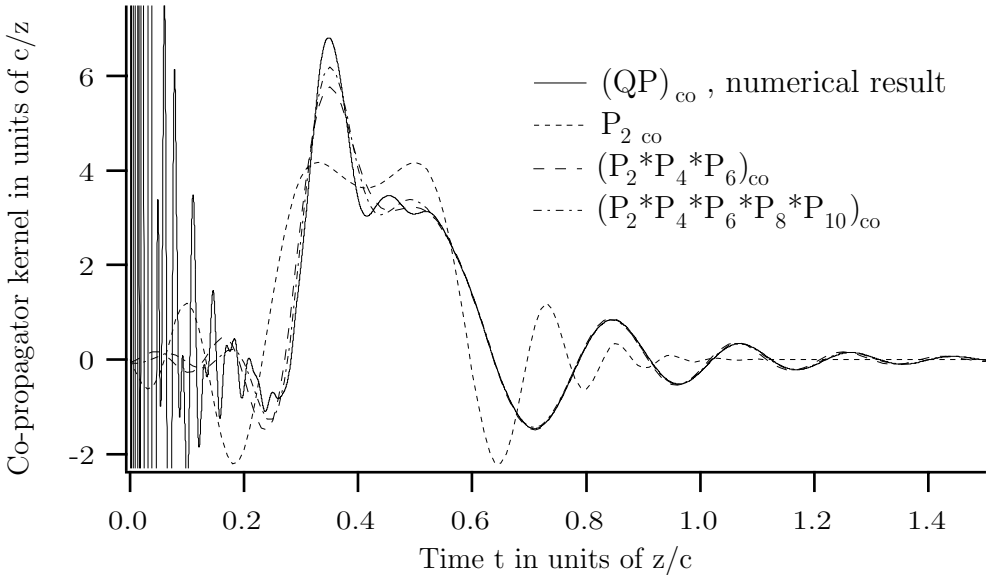

Figure 4: The co-propagator kernel, $(QP)_{\rm co}(z,t) = {\rm Re}\{Q_c(z)P_c(z;t)\}$, at a fixed propagation depth, z, in a gyrotropic medium ($\omega_p = 100 \times c/z$, $\omega_0 = 100 \times c/z$, $\omega_g = 100 \times c/z$, $\nu = 20 \times c/z$). 32768 data points were used at the equidistant discretization of the time interval $0 < t < 1.5 \times z/c$. The leading-edge behavior is characterized by high amplitudes ($\approx 5000 \times c/z$). Second precursor approximations obtained by the time-domain method are shown also.

Appendix A The hyper-Airy functions $A_{2k}(z)$

This appendix concerns hyper-Airy functions of even order and complex argument. Hyper-Airy functions of real arguments were introduced in Ref. 11.

Definition A.1. *Let k be an arbitrary positive integer. The function $A_{2k}(z)$ of complex argument z is the inverse Fourier transform of the function* $\exp\left(-\xi^{2k}/(2k)\right)$ *extended to an entire function on the whole complex plane. (Fourier-Laplace transform; see Ref. 9). Explicitly,*

$$A_{2k}(z) = \frac{1}{2\pi} \int\limits_{-\infty}^{\infty} \exp\left(-\xi^{2k}/(2k) + iz\xi\right) d\xi, \quad z \in \mathbb{C}. \tag{A.1}$$

The hyper-Airy functions $A_{2k}(z)$ are even in z. Setting $k = 1$ gives the Gaussian function $A_2(z) = \exp\{-z^2/2\}/\sqrt{2\pi}$.

Differentiating under the integral sign yields the ordinary differential equations

$$A_{2k}^{(2k-1)}(z) = (-1)^k z A_{2k}(z), \quad z \in \mathbb{C}, \quad k > 0. \tag{A.2}$$

From Ref. [11, Appendix B], one obtains the initial values

$$A_{2k}^{(2m)}(0) = \frac{(-1)^m}{\pi}(2k)^{\frac{2m+1}{2k}-1}\Gamma\left(\frac{2m+1}{2k}\right), \quad A_{2k}^{(2m-1)}(0) = 0, \tag{A.3}$$

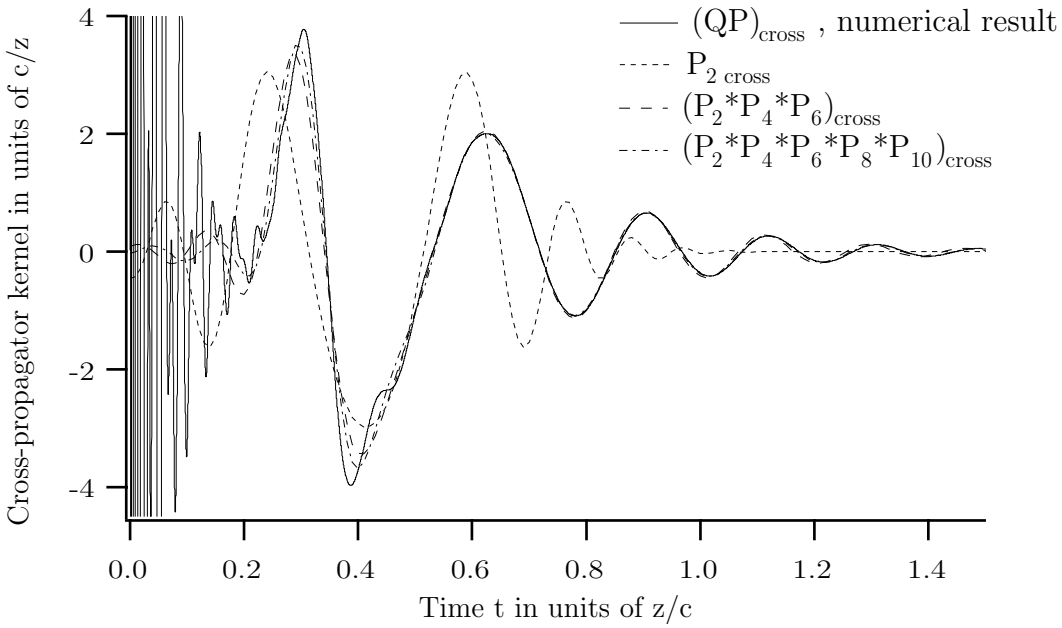

Figure 5: The cross-propagator kernel, $(QP)_{\text{cross}}(z,t) = \text{Im}\{Q_c(z)P_c(z;t)\}$, and second precursor approximations to this kernel at a fixed propagation depth, z, in a gyrotropic medium. For parameters see caption of Figure 4. The leading-edge behavior is characterized by amplitudes of order $100 \times c/z$.

where $\Gamma(x)$ is the gamma function. Restrictions of the functions $A_{2k}(z)$ to the ray $[0, +\infty u)$, where $0 \neq u \in \mathbb{C}$ is arbitrary but fixed, can be obtained by solving the hyper-Airy equations (A.2) subjected to the initial values (A.3). In the vicinity of the origin, standard ODE-solvers can be used.

Alternatively, convolution equations for the hyper-Airy functions, which are obtained by repeated integration of equations (A.2), can be solved:

$$A_{2k}(z) = \frac{(-1)^k}{(2k-2)!}\int_C (z-\xi)^{2k-2}\xi A_{2k}(\xi)\,d\xi + \sum_{m=0}^{2k-2}\frac{x^m}{m!}A_{2k}^{(m)}(0), \tag{A.4}$$

where C is the segment, $[0, z]$, $z \in \mathbb{C}$. These Volterra equations of the second kind are uniquely solvable in the space of continuous functions on each finite segment.

The leading behavior of the hyper-Airy functions, $A_{2k}(z)$, $k > 1$, as $|z| \to \infty$ is

$$\begin{aligned} A_{2k}(z) \sim \frac{(jz)^{-\frac{2k-2}{2(2k-1)}}}{\sqrt{2\pi(2k-1)}}\Bigg(&\exp\left(\frac{2k-1}{2k}(jz)^{\frac{2k}{2k-1}}\right) \\ &+(-1)^{-\frac{2k-2}{2(2k-1)}}\exp\left(\frac{2k-1}{2k}(-jz)^{\frac{2k}{2k-1}}\right)\Bigg), \end{aligned} \tag{A.5}$$

cf. the analysis in Ref. 11 (see also [2, Chapter 6]). This result is not applicable to the Gaussian function, $A_2(z)$. It is possible to improve the expansion (A.5) by retaining more terms in the asymptotic series of $A_{2k}(z)$ as $|z| \to \infty$, cf. Ref. 11.

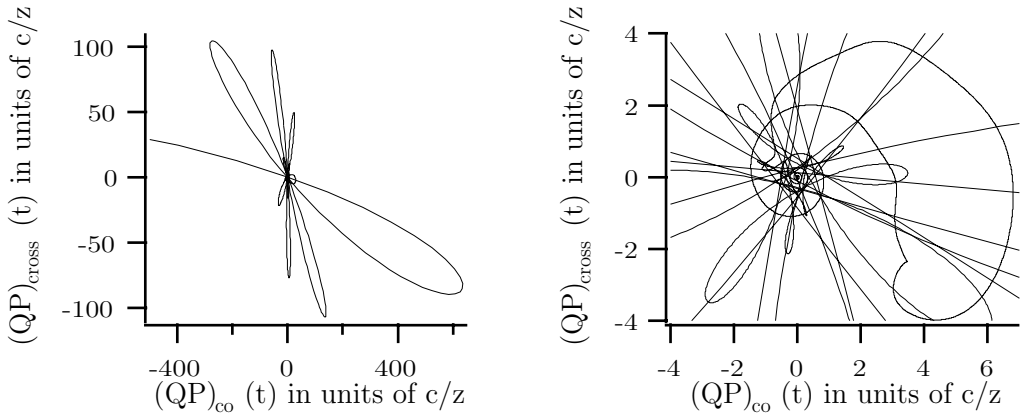

Figure 6: Polar plot of $(QP)_{\text{cross}}(z,t)$ versus $(QP)_{\text{co}}(z,t)$ with time as the parameter at a fixed propagation depth, z, in a gyrotropic medium; (a) general view; (b) detailed view that reveals the second forerunner. The wave travels towards the reader.

References

[1] E. Beltrami. Considerazioni idrodinamiche. *Rend. Inst Lombardo Acad. Sci. Lett.*, **22**, 122–131, 1889.

[2] C. M. Bender and S. A. Orszag. *Advanced Mathematical Methods for Scientists and Engineers*. McGraw-Hill, New York, 1978.

[3] L. Brillouin. Über die Fortpflanzung des Lichtes in dispergierenden Medien. *Ann. Phys.*, **44**, 203–240, 1914.

[4] L. Brillouin. *Wave propagation and group velocity*. Academic Press, New York, 1960.

[5] E. U. Condon. Theories of optical rotatory power. *Rev. Mod. Phys.*, **9**, 432–457, 1937.

[6] P. Drude. *Lehrbuch der Optik*. S. Hirzel, Leipzig, 1900.

[7] C. Eftimiu and L. W. Pearson. Guided electromagnetic waves in chiral media. *Radio Sci.*, **24**(3), 351–359, 1989.

[8] J. Fridén and G. Kristensson. Transient external 3D excitation of a dispersive and anisotropic slab. *Inverse Problems*, **13**, 691–709, 1997.

[9] L. Hörmander. *The Analysis of Linear Partial Differential Operators I*. Grundlehren der mathematischen Wissenschaften 256. Springer-Verlag, Berlin Heidelberg, 1983.

[10] A. Karlsson and G. Kristensson. Constitutive relations, dissipation and reciprocity for the Maxwell equations in the time domain. *J. Electro. Waves Applic.*, **6**(5/6), 537–551, 1992.

[11] A. Karlsson and S. Rikte. The time-domain theory of forerunners. *J. Opt. Soc. Am. A*, **15**(2), 487–502, 1998.

[12] H.-O. Kreiss and J. Lorenz. *Initial-Boundary Value Problems and the Navier-Stokes Equations*. Academic Press, San Diego, 1989.

[13] R. Kress. *Linear Integral Equations*. Springer-Verlag, Berlin Heidelberg, 1989.

[14] G. Kristensson and S. Rikte. Transient wave propagation in reciprocal bi-isotropic media at oblique incidence. *J. Math. Phys.*, **34**(4), 1339–1359, 1993.

[15] I. V. Lindell. *Methods for Electromagnetic Field Analysis*. Clarendon Press, Oxford, 1992.

[16] I. V. Lindell, A. H. Sihvola, S. A. Tretyakov, and A. J. Viitanen. *Electromagnetic Waves in Chiral and Bi-isotropic Media*. Artech House, Boston, London, 1994.

[17] I. V. Lindell, S. A. Tretyakov, and A. J. Viitanen. Plane-wave propagation in a uniaxial chiro-omega medium. *Microwave Opt. Techn. Lett.*, **6**(9), 517–520, 1993.

[18] S. A. Maksimenko, G. Y. Slepyan, and A. Lakhtakia. Gaussian pulse propagation in a linear, lossy chiral medium. *J. Opt. Soc. Am. A*, **14**(4), 894–900, 1997.

[19] M. Norgren and S. He. Electromagnetic reflection and transmission for a dielectric-Ω interface and a Ω slab. *Int. J. Infrared and MM Waves*, **15**(9), 1537–1554, 1994.

[20] M. Norgren and S. He. Reconstruction of the constitutive parameters for an Ω material in a rectangular waveguide. *IEEE Trans. Microwave Theory Tech.*, **43**(6), 1315–1321, 1995.

[21] K. E. Oughstun and G. C. Sherman. Propagation of electromagnetic pulses in a linear dispersive medium with absorption (the Lorentz medium). *J. Opt. Soc. Am. B*, **5**(4), 817–849, 1988.

[22] K. E. Oughstun and G. C. Sherman. *Electromagnetic Pulse Propagation in Causal Dielectrics*. Springer-Verlag, Berlin Heidelberg, 1994.

[23] S. Rikte. Sommerfeld's forerunner in stratified isotropic and bi-isotropic media. Technical Report LUTEDX/(TEAT-7036)/1–26/(1994), Lund Institute of Technology, Department of Electromagnetic Theory, P.O. Box 118, S-211 00 Lund, Sweden, 1994.

[24] S. Rikte. The Theory of the Propagation of TEM-Pulses in Dispersive Bi-isotropic Slabs. Technical Report LUTEDX/(TEAT-7040)/1–22/(1995), Lund Institute of Technology, Department of Electromagnetic Theory, P.O. Box 118, S-211 00 Lund, Sweden, 1995.

[25] M. M. I. Saadoun and N. Engheta. A reciprocal phase shifter using noval pseudochiral or Ω medium. *Microwave Opt. Techn. Lett.*, **5**(4), 184–187, 1992.

[26] S. Shen and K. E. Oughstun. Dispersive pulse propagation in a double-resonance Lorentz medium. *J. Opt. Soc. Am. B*, **6**(5), 948–963, 1989.

[27] A. H. Sihvola and I. V. Lindell. Material effects in bi-anisotropic electromagnetics. *IEICE Transactions of Electronics (Japan)*, **E78-C**(10), 1383–1390, 1995.

[28] A. Sommerfeld. Über die Fortpflanzung des Lichtes in dispergierenden Medien. *Ann. Phys.*, **44**, 177–202, 1914.

[29] J. A. Stratton. *Electromagnetic Theory.* McGraw-Hill, New York, 1941.

[30] P. G. Zablocky and N. Engheta. Transients in chiral media with single-resonance dispersion. *J. Opt. Soc. Am. A*, **10**(4), 740–758, 1993.